

Article

Automated Reconditioning of Thin Wall Structures Using Robot-Based Laser Powder Coating

Shahram Sheikhi ^{1,*}, Eduard Mayer ¹, Jochen Maaß ² and Florian Wagner ³

¹ Department Mechanical Engineering and Production, Institute for Materials Science and Welding, Berliner Tor 13., 20099 Hamburg, Germany; eduard.mayer@haw-hamburg.de

² Department Informations-und Elektrotechnik, Berliner Tor 7, 20099 Hamburg, Germany; jochen.maass1@haw-hamburg.de

³ Gall and Seitz Systems GmbH, Vogelreth 2-4, 20457 Hamburg, Germany; Wagner@gall-seitz.com

* Correspondence: shahram.sheikhi@haw-hamburg.de

Received: 14 January 2020; Accepted: 10 February 2020; Published: 17 February 2020



Abstract: Implementing digitalization in the field of production represents a major hurdle for some small- and medium-sized enterprises (SMEs) due to the ensuing demands on employees and, in some cases, the significant financial investment required. The RobReLas research project has developed a system whose purpose is to enable an economical solution to this dilemma for SMEs in the field of automated, robot-based reconditioning of components. A laser scanner was integrated in the robot's control. The data generated by the scanner are used to mathematically describe the virtual area of the surface to be laser-treated. The scanner recognizes the relevant area within the robot's predefined work space by defining the maximum length and width of the relevant component. The system then automatically applies predefined and qualified repair strategies in the virtual area. Tests on nickel-based blades demonstrated the system's economic potential, showing a reduction in reconditioning time of about 70% compared to the conventional reconditioning method. The main advantage of the system is the fact that a basic knowledge of operating robots is sufficient for the attainment of repeatable results. Further, no additional CAD/CAM workstations are required for implementation.

Keywords: digitalization; robotic application; reconditioning; welding; laser

1. Introduction

Today's businesses face the challenge of developing and implementing new strategies and innovations in order to consistently produce high-quality and efficient products and, therefore, meet rising customer expectations and succeed in increasingly competitive globalized markets. In this context, the development of innovative methods and processes via digitalization promises productive results. Digitalization enables the intelligent automation of previously labor-intensive manual work, which helps compensate for the issues raised by the current shortage of skilled workers. Reconditioning by means of welding/surfacing of components is a traditional area of production [1]. The quality of the repair achieved depends, to a significant degree, on employee qualifications and experience. As well as conducting purely manual repair processes, employees need to operate a handling system (robots or portal systems), while also being skilled in the field of welding as a repair method.

Parts within turbomachines that experience particular levels of stress are found in compressors and turbine blades. In the event of damage, repair is often cheaper than replacement. With regard to ship parts in particular, the purchase of new components often entails delivery times—and therefore idle periods—of several months. A repaired part is often over 50% cheaper than a new purchase; for this reason, industrial businesses are increasingly attempting to use automated processes for reconditioning

damaged machine components. The prerequisite for automated reconditioning, however, is the knowledge or recording of the actual geometry, i.e., the actual shape and dimensions, of the entire component, or at least of the body to be welded [2,3].

Three methods of reconditioning job automation are available. The surface of thin-walled structures to be reconditioned is usually determined manually using the so-called teach-in process. This procedure is extremely time-consuming and sometimes accounts for 80% of total working time. The time required increases in proportion with the complexity of the geometry to be captured. Further, a serious drawback to this methodology is the major impact on welding quality—potentially leading to failure during welding—caused by even the smallest inaccuracy in teaching. In addition, research has shown that the positioning of teaching is always dependent on the employee performing the procedure and his or her form on the day. This results in potential sources of failures and reduces the repeatability of the quality achieved.

Another method of automated reconditioning uses tactile sensors, which involves manual scanning of the surface to be reconditioned, given sufficiently high accuracy of the handling system. The data attained feed into the development of a corresponding program. This type of automation is preferable where a limited number of different geometries are present, as each geometry requires an individual program to scan the surface. In addition, the clamping system is particularly important in this process, as the constant position of the components is vital. The third method which finds industrial use requires a scanner solution and CAD/CAM systems. This robot-based digitization of surfaces is state-of-the-art, provided that the handling system has the necessary accuracy. A scanner digitizes each location, and an additional CAD program processes the data. In the CAD program, the employee selects the areas to be rearranged, then a corresponding program is created and transferred to the control of the handling system. The application of this method to the reconditioning of thin wall structures characterized by short welding times, low quantities, and high product diversity does not appear commercially feasible (for small- and medium-sized enterprises (SMEs)), as it requires comparatively high investment in CAD/CAM systems and an additional workstation for data processing and control of the program [4,5].

Jones et al. describe a remanufacturing system of turbine blades by laser cladding, machining, and in-process scanning, which is very much comparable to the approach followed within the aim of RobReLas. They automated the remanufacturing process of the blades by gelling together functionality of a software suite which includes reverse engineering, fixturing, inspection, CAD and CAM applications (PowerSHAPE, Fixture, PowerINSPECT, and PowerMILL). For the blade re-tipping application, the scanned points are captured by PowerINSPECT (using Fixture to avoid any collisions) and then translated via PowerSHAPE into a virtual model of the actual 3D geometry. The nominal CAD model is then morphed by PowerSHAPE based on the actual geometry measurements to provide a pseudo-real-time virtual representation of the part as it progressed through the reconditioning steps, from which adaptive tool paths are generated by PowerMILL for defect removal, cladding, milling, and blending operations [6]. However, the necessity of software suites and the limitation of the described system to blade applications are the main differences to RobReLas.

A comparison of the existing solutions as described above illustrates the need for an economical automation solution for SMEs. The typical manual variant is a simple solution, but not economical due to labor costs. The introduction of tactile sensors requires programming knowledge, especially when components do not meet the standard. Implementing CAD/CAM solutions is not a persuasive solution for SMEs due to the expense required, specifically the need for additional workstations to operate the software, the cost of annual licensing fees, and the higher demands placed on operators. There is therefore a need for research around the development of applied digitization solutions appropriate to user needs. Section 2 of this paper delineates the equipment required. Section 3 outlines the methods for detection of the surface to be processed, i.e., the surface of the component to be reconditioned, and the calculations for the welding paths. Section 4 explores the applicability of the system to a turbine blade and a steel bar and discusses optimization solutions for the beginning of the welding process.

2. Experimental Setup

The present research project used an industrial robotic arm of type KUKA KR 125/3, controlled by a KR C2 controller. It is a 6 DOFs robotic arm with a payload of 125 kg, maximum reach of 2410 mm and a repeatability of ± 0.2 mm. A turning and tilting table is attached to the robot, providing 2 extra DOFs.

The method of reconditioning used is called laser powder welding. This method is also used for additive manufacturing of components and is known as LMD (Laser Metal Deposition). Essentially, a defocused laser beam (laser spot) is directed to the surface of the component. At the same time, pulverized material is supplied through a nozzle into the laser spot. The energy density of the laser melts the powder (coating material) and the base material. Argon is used to carry the powder onto the workpiece and simultaneously protects the melt pool from reacting with atmospheric gases. The laser spot and the powder nozzles are guided over the surface of the specimen along a predefined path, resulting in a weld bead (Figure 1). The surface of the workpiece is coated by offsetting the weld bead in the plane, as described below. The system is then moved upwards by the resulting layer height and the process is repeated until the required number of layers, and thus the required layer height, has been reached.

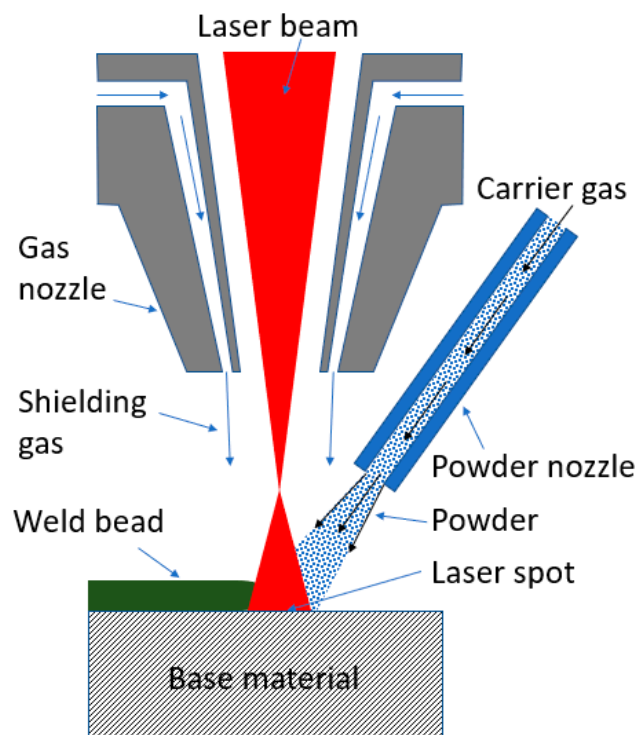


Figure 1. Schematic visualization of the laser metal deposition (LMD) process.

A commercially available laser scanner made by Micro Epsilon detected the surface to be reconditioned. As described on the homepage of Micro Epsilon [6], “The laser scanner uses the laser triangulation principle for two-dimensional profile detection on different target surfaces. By using special lenses, a laser beam is enlarged to form a static laser line and is projected onto the target surface (red line on the specimen in Figure 1). The optical system projects the diffusely reflected light of this laser line onto a highly sensitive sensor matrix. In addition to distance information (z-axis), the controller also uses this camera image to calculate the position along the laser line (x-axis). These measured values are then output in a two-dimensional coordinate system that is fixed with respect to the sensor. In the case of moving objects or a traversing sensor, it is therefore possible to obtain 3D measurement values.” The mentioned description is depicted in Figure 2.

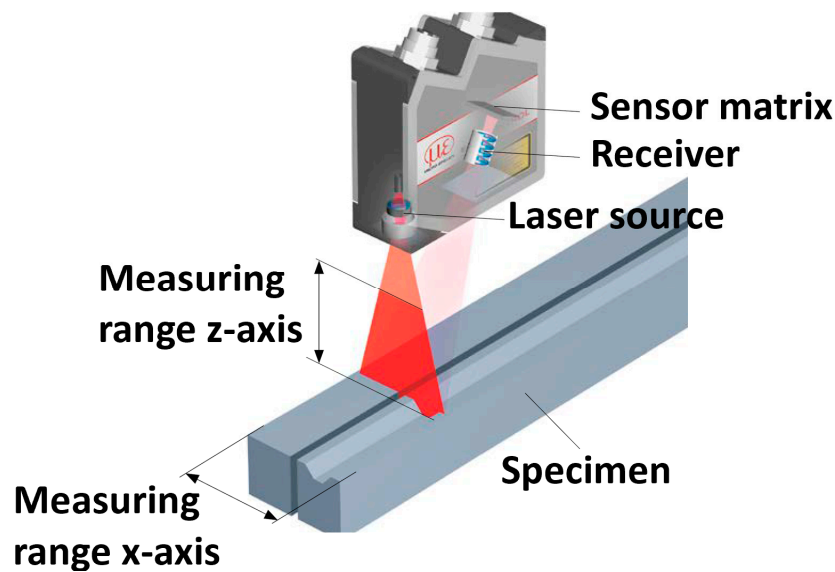


Figure 2. Laser scanner system based on laser light triangulation [6].

The technical specification of the scanner is the following:

- z-axis measuring range: 290 mm
- x-axis measuring range: 120 mm
- Profile frequency: up to 4.000 Hz
- Measuring rate: up to 2.560.000 points/sec
- z-axis reference resolution: 12 μm
- x-axis resolution: 1.280 points/profile
- Permissible ambient light: 10.000 lx
- Laser source: semiconductor laser 658 nm (red)
- Laser power: 8 mW (class 2M)

This scanner enables internal data preprocessing without the need for additional software. The system is first configured in accordance with the desired selection criteria, such as maximum or minimum value. Automatic data acquisition in accordance with the selected criteria then takes place. Further, this system has an interface suitable for integration of the scanner into the robot's control, which makes this integration process less complex and reduces the cost of the investment.

The laser scanner was integrated into the robot's control. In order to integrate the scanner into the welding head, a construction was created with an appropriate level of stability and robustness alongside flexibility which allows for the scanner to be set up and dismantled as necessary (Figure 3). It is important to ensure that vibrations from the robot's motion profile do not affect the location of the scanner. In addition, the scanner must be protected from exposure to heat during the welding process in order to avoid thermal congestion of the sensors. For this purpose, an integrated pneumatic protective device was designed to shield the scanner during welding. Typically, the sensor is protected from thermal stress due to an offset between the scanning beam and the melting bath. However, this offset can negatively affect the accuracy of repositioning in the case of filigree components, and therefore needed to be avoided in this project.

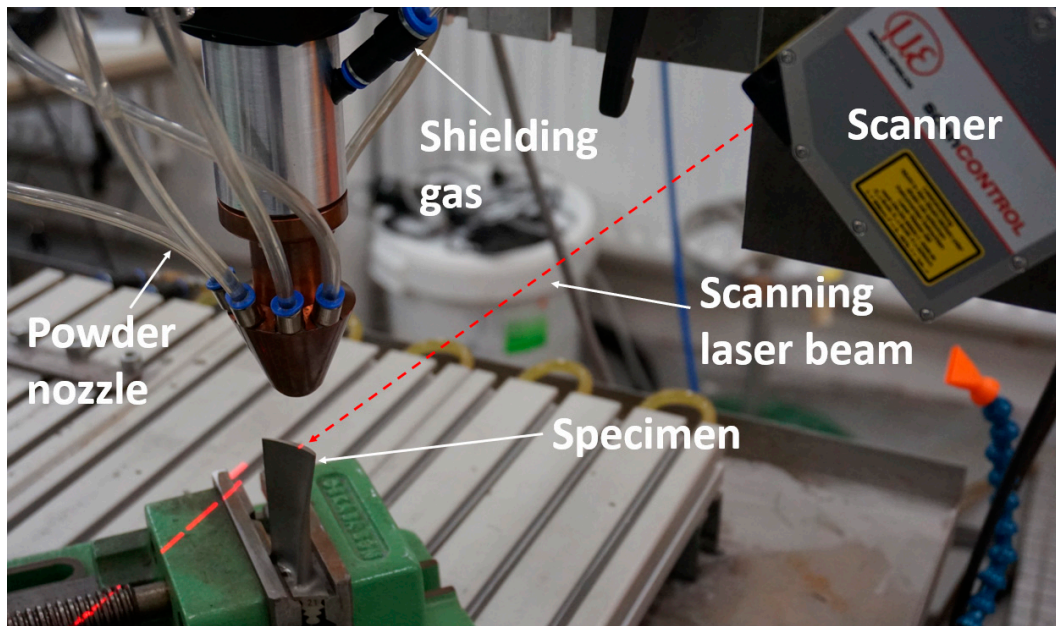


Figure 3. Setup of the scanning and welding head.

3. Technical Solution

The reproducibility of the reconditioning result depends on the accuracy of the handling system. At the outset of the project, a reference sample with a defined point pattern was created. The points of the pattern were approached with the tool center point (TCP) of the robot and the difference between the coordinates of the points approached, and the point pattern was determined. Corrective factors were calculated from the differences identified, enabling subsequent adjustment of the TCP's location. The deviations in accuracy produced by the robot were compensated procedurally; this entailed the testing of different robot paths in order to minimize the influence of the 6 axes on positioning accuracy when reaching the starting and end points. This allowed the definition of a working space with a repetitive accuracy of 0.05 mm. The coordinate systems are calibrated to enable the transformation into each other of the different systems of coordinates of the laser scanner and the robot. For this purpose, a calibration tool was designed to the end of creating a mathematical relationship between the coordinates measured by the scanner and the robot coordinates. The coordinates determined by the scanner were automatically transformed using the robot programming language and then used to define the robot's path. The first step of the reconditioning process entails the automated detection of the surface to be processed. Figure 4a shows the surface being scanned. All points in the scanning beam are recorded (Figure 4b). The highlighted dots correspond to the relevant area of the scanning beam, in accordance with the right-hand image in Figure 4c, which shows the position of the laser beam on the area.

As indicated above, one of the disadvantages of automated systems is the necessity of an additional workstation for the processing of data. For this reason, all necessary mathematical operations for the description of the relevant plane in each case were handled in the context of the robotic programming language KRL. KRL offers limited opportunities for performing mathematical operations. A database or library for mathematical operations was therefore created using KRL. This database includes subprograms with mathematical functions such as:

- Calculate vector length;
- Calculate a unit vector;
- Form a scalar product;
- Add and subtract vectors;

Square;
 Calculate natural logarithms;
 Inverse function.

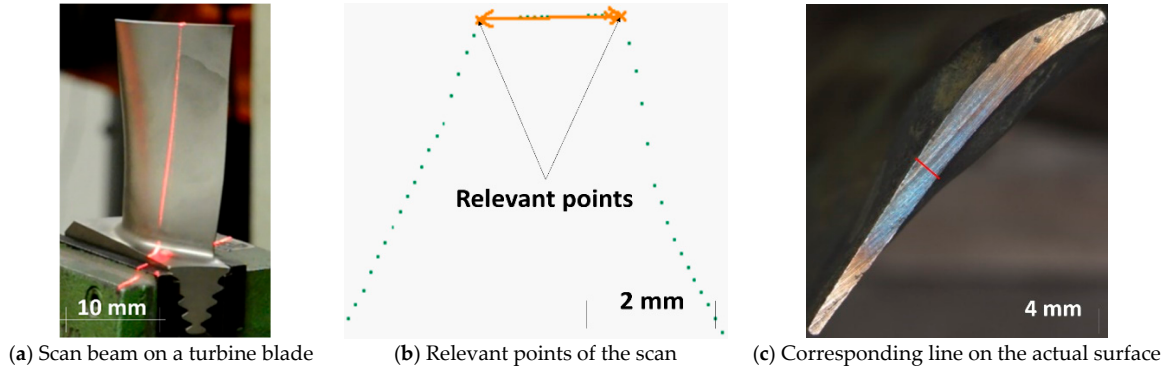


Figure 4. The scanning process.

A program was written to process and store the data that the scanner constantly transmits to the controller. This program records contour points every 0.1 mm during the scan phase, which allows the storage of 10 measuring points for a Section 1 mm thick. If the number of stored points is not sufficient for accurate capture of the component’s contours, the program enables easy changes to this setting. The values scanned in this way are stored in an array and are directly accessible to the robot. Further, a displacement (Δy) was defined of the TCP to the outer edge of the part to be scanned in each case, enabling operators to subsequently manually shift the contour as calculated. To accurately capture the starting and end point of the component, the scanning process starts with a certain distance to the actually relevant point for welding and stops beyond the relevant end point for welding (Figure 5). An algorithm was written for the purpose of calculating the starting and end point of the component’s relevant area.

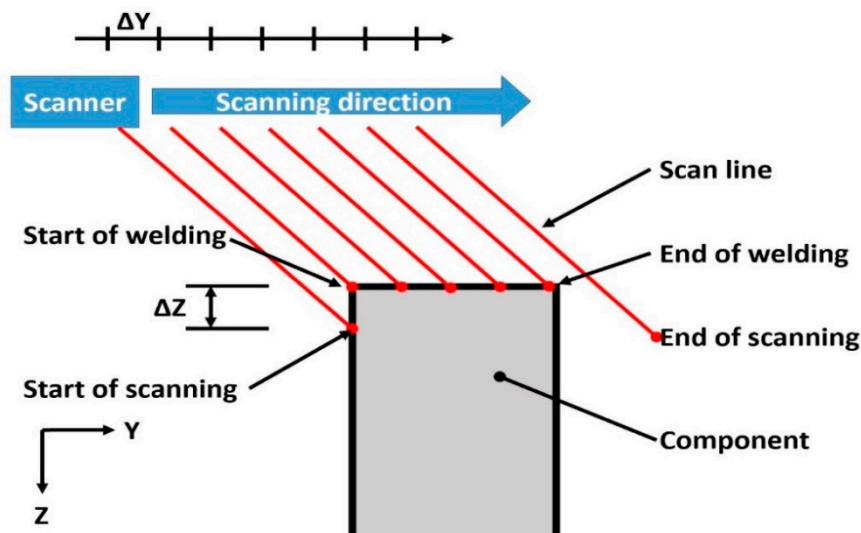


Figure 5. Identifying the starting point.

For this purpose, the slope of neighboring points was determined. The first calculated slope with a value of less than 0.3 enabled identification of the starting point and the deletion of all previous points. A program for smoothing the scanned and processed points was developed to suppress noise and eliminate irregularities in the readings. This involved the application of a customized Savitzky

Golay filter, which, unlike other smoothing filters, does not simply cut off specific proportions of high frequencies or deviations, but includes them in the calculation. Thus, the filter demonstrates excellent properties of distribution, such as relative maxima, minima, and scattering, which are usually distorted by conventional methods, such as the formation of the moving mean by flattening or displacement [7,8].

Thus far, a virtual plane of the surface could be generated in the robot's control using KRL. The next step consists of a method for the automatic calculation of a path for the welding process. Experiments have shown that shifting one of the boundaries of the virtual area to a predefined offset generates best-quality results. The offset was found to be 50% of the width of the weld seam. The program's operator is able to adjust the offset if necessary and decide which side of the contour has to be shifted in parallel.

In contrast to existing digitalization solutions with CAD/CAM, the user does not see an image of the digitalized surface. Therefore, before starting the actual welding, the operator may choose to simulate it, that is, to run the movement of the TCP without switching on the laser and powder. The operator observes the movement through an integrated camera in the laser optic, checking the location of the calculated tracks, and can, if necessary, adjust the path by using corrective factors in the x and y directions. This has made it possible for the first time to implement a fully automated solution without the establishment of further CAD/CAM workstations and without needing an employee with specific programming skills.

A mathematical description of the welding process is necessary to develop the automated welding strategy using laser powder coating (LPC). LPC results in weld beads with a height H and width ω , which correlate with applied welding parameters. Since LPC is a dynamic process, the weld material dilutes into the base material. The resulting dilution is expressed by the depth h and highly depends on the heat input of the process and the powder feed rate. The resulting material is a metallurgical mixture of the base material and weld material which results in a strong bond between the build-up structure and the component [9–15]. Depending on welding parameters, the geometrical shape of the weld bead, as well as the dilution depth, vary. LPC requires numerous parameters in order to define values for the automation process. For a better evaluation of the process parameter correlation, the following theoretical equations and assumptions are established.

The overlapping ratio μ_c , which is indicated in Figure 6 and predominantly determined by an adjustment of the bead spacing dc , has to be considered. To examine the resulting surface roughness for the estimated values of dc , four different bead distances, ranging from 0.25 mm to 1.5 mm, were used. Depending on the laser spot diameter $d_L(z)$ and powder spot diameter $d_p(z)$, the overlapping ratio μ_c varies. Since d_L and d_p highly influence H , h , ω , and α of the weld bead, they adjust the overlapping ratio μ_c as well. Internal preliminary studies have been performed to find optimum spot sizes for the laser and the powder. The spot size correlates with the distance of the welding head relative to the surface of the base material. The laser spot diameter $d_L(z)$, e.g., is described by Equation (1) as a function of the Rayleigh length z_r , and the defocusing distance, which is reduced by z relative to the optic-specific smallest focal spot diameter d_f .

$$d_L(z) = d_f \times \sqrt{1 + \left(\frac{z}{z_r}\right)^2} \quad (1)$$

According to [13], the overlapping ratio μ_c of the beads is defined as:

$$\mu_c = \frac{(\omega - dc)}{\omega} \quad (2)$$

For later quality assurance, it is important to determine the theoretical aspect ratio R_B , which is quotient of bead width ω and bead height H ,

$$R_B = \frac{\omega}{H} \quad (3)$$

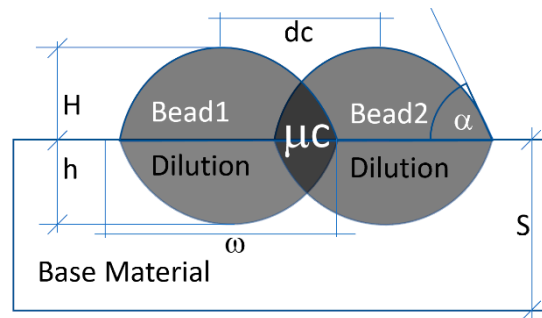


Figure 6. Overlapping weld beads.

For the improvement of the surface quality in the coating process, a circularly shaped bead is assumed according to [13]. In order to reduce the surface roughness after a multilayer LPC process, a certain bead spacing, $d_c > 0$ and $d_c < \omega$, have been defined, resulting in a smooth surface when both Sections, S1 and S2, are of equal sizes, Figure 7.

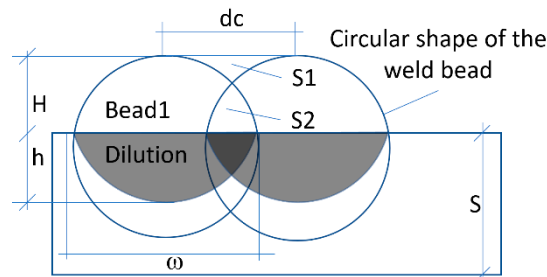


Figure 7. Theoretical shape of the weld bead.

The radius R of the circular shape of the weld bead is calculated by considering the height H and width ω of the bead. According to [14], the radius can be expressed by

$$R = \frac{(\omega^2 + 4 \times H^2)}{8 \times H} \tag{4}$$

The size of the areas S_1 and S_2 according to [14] are determined as:

$$S_1 = R \times d_c - R^2 \times \arcsin\left(\frac{d_c}{2 \times R}\right) - \frac{d_c}{2} \times \sqrt{R^2 - \left(\frac{d_c}{2}\right)^2} \tag{5}$$

$$S_2 = \left(R^2 \times \arcsin\left(\frac{\omega}{2 \times R}\right) + \frac{\omega}{2} \times \sqrt{R^2 - \left(\frac{\omega}{2}\right)^2}\right) - \left(R^2 \times \arcsin\left(\frac{d_c}{2 \times R}\right) + \frac{d_c}{2} \times \sqrt{R^2 - \left(\frac{d_c}{2}\right)^2}\right) + (H - R) \times (\omega - d_c) \tag{6}$$

The dilution is the degree of material mixture resulting from the molten base material and powder during the laser cladding process. Assuming a circularly geometric shape of the bead as well as for the molten zone of the base material, [15] expresses the dilution as

$$\eta = \frac{\left[\left[\frac{\left(\frac{\omega}{2}\right)^2 + h^2}{h \times \omega}\right] \times \arcsin\left[\frac{h \times \omega}{\left(\frac{\omega}{2}\right)^2 + h^2}\right] - \left[\left(\frac{\omega}{2}\right)^2 - h^2\right]\right]}{\left[\frac{h \times \left[\left(\frac{\omega}{2}\right)^2 + H^2\right]^2}{\omega \times H^2}\right] \times \arcsin\left[\frac{\omega \times H}{\left[\left(\frac{\omega}{2}\right)^2 + H^2\right]^2}\right] + \left[\frac{\left(\frac{\omega}{2}\right)^2 + h^2}{\omega \times h}\right] \times \arcsin\left[\frac{\omega \times h}{\left(\frac{\omega}{2}\right)^2 + h^2}\right] - \frac{\left[\left(\frac{\omega}{2}\right)^2 - H \times h\right] \times (H + h)}{H}} \tag{7}$$

Taking into account only the maxima of dilution and the bead height, the dilution ratio can be simplified to

$$\eta_{max} = \frac{h}{(H + h)} \quad (8)$$

The length of a weld bead (L) is determined by the calculated virtual plane. The length varies depending on the position to be welded. However, a constant welding velocity vt is necessary to assure the same bead geometry and, by that, the same coating quality. Using the velocity v_t and the length of a bead, the process time (t) of each bead is calculated according to Equation (9).

$$t = \frac{L}{v_t} \quad (9)$$

In addition to the welding speed and the bead length, it is important to control the powder feed rate (m), which depends on the material density and its grain size. For each material and grain size, calibrated parameters for powder transportation have been experimentally evaluated. It is necessary to apply the same amount of powder on a specific weld length. Therefore, the ratio (m') of powder feed rate and velocity has been used to control the system, Equation (10).

$$m' = \frac{m}{v_t} \quad (10)$$

4. Results

This solution was applied to a variety of geometries. Figure 8 shows two examples of components (a rectangular cross-sectional surface in Figure 8a and a turbine blade in Figure 8b) being reconditioned using Inconel 625 (nickel-based alloy with 21% Cr and 8.5% Mo as the main alloying elements). The program allows users to store different types of components in a database with their corresponding scanning and welding parameters. Figure 8 shows automatically regenerated components, with a non-reconditioned area visible on the left-hand side of the images. These failures resulted from the communication of the laser control with the controls of the robot.

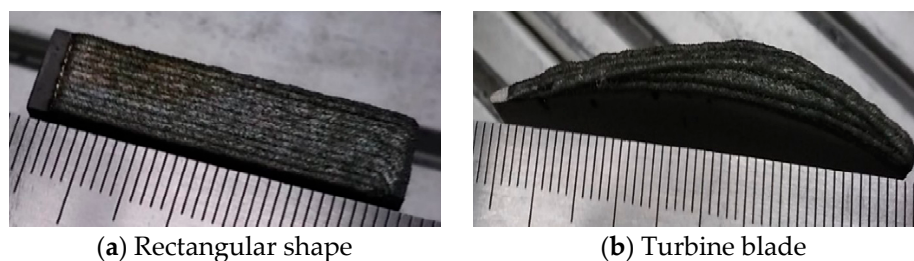


Figure 8. Automatically regenerated components.

An important factor influencing the quality of the reconditioning process is the time lag generated by switching the laser on and off. It was therefore necessary to experimentally determine the time delay between the command 'laser on' and the actual impact of the laser on the surface. For this purpose, an experiment was carried out in which four lanes of the same length were welded at different speeds (see Figure 9). The switch-on signal was programmed identically on all four tracks. The predetermined length of the path was 60 mm and the switch-on signal for the laser was activated after 20 mm of travel. The welded track was then surveyed and the delay was calculated. The mean delay between the switch-on signal and the impact of the laser beam was 0.2 s.

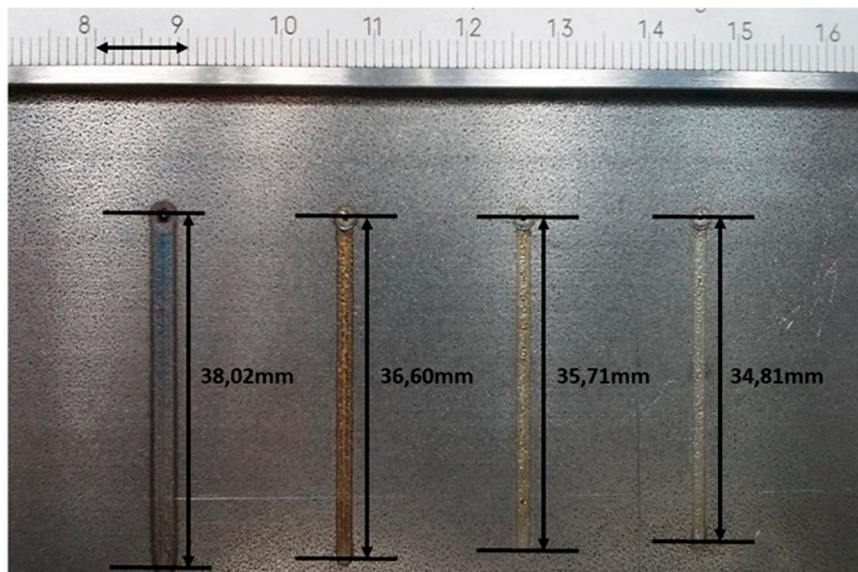


Figure 9. Setup for establishing time delay.

After adjusting the time delay, sound welds could be produced, as shown in Figure 10; this eliminates starting failure at the beginning of the welding process. Figure 10a shows the result of the system applied to a rectangular shape and Figure 10b to a real turbine blade.

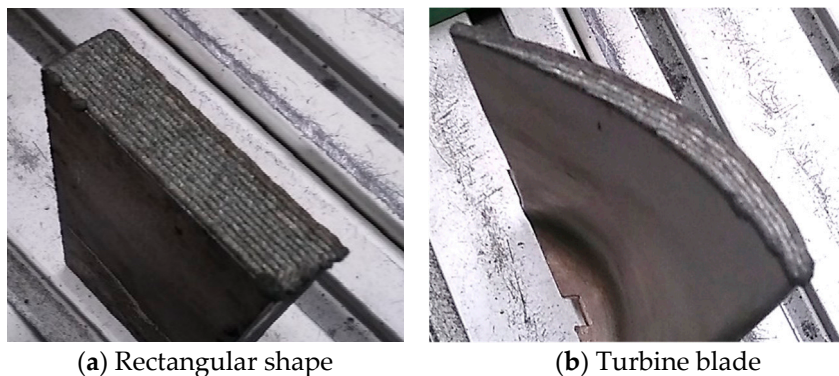


Figure 10. Automatically regenerated components with optimized parameters.

After optimization of the welding parameters, sound welds were produced using the following parameters:

- Laser power: 450 W
- Travelling speed: 1.2 m/min
- Spot diameter: 1 mm
- Powder rate: 12 g/min
- Weld pitch: 0.5 mm
- 10 layers

Hardness distribution from the base material to the middle of the weldment is depicted in Figure 11. The hardness of the weldment (range: -2 to -0.5) is about 262 HV1 and is lower than that of the base material (range: 0.5 to 1.5). This distribution matches that observed in conventionally reconditioned blades using the teach-in method (see sample S1 in Figure 11). Samples S10, S26, and S28 refer to blades with different thicknesses that were reconditioned automatically. Depending on the

powder deployed, mismatch between weldment and base material is avoidable. However, a hardening effect is invariably observed in the heat-affected zone.

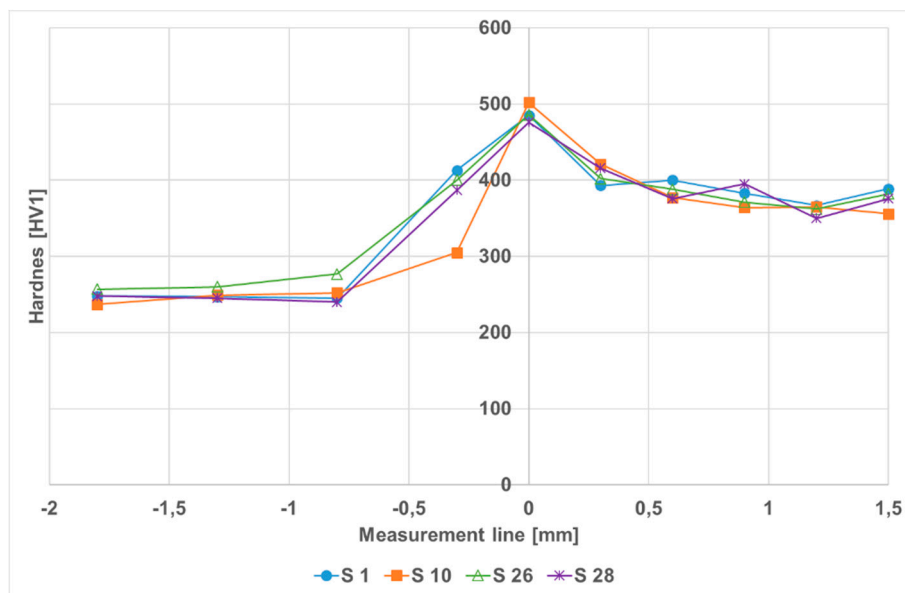


Figure 11. Hardness distribution.

Depending on the damage sustained by the components, multiple layers are required for their reconditioning. Within the course of this research, a total height of 6 mm was regenerated. The quality of the regenerated area was examined using optical microscopy. Figure 12c shows a cross-section of a reconditioned blade. Minor pores with diameters of 15 to 30 μm are evident (see Figure 12a,b), but their limited number, their spherical shape, and size permit their classification as acceptable.

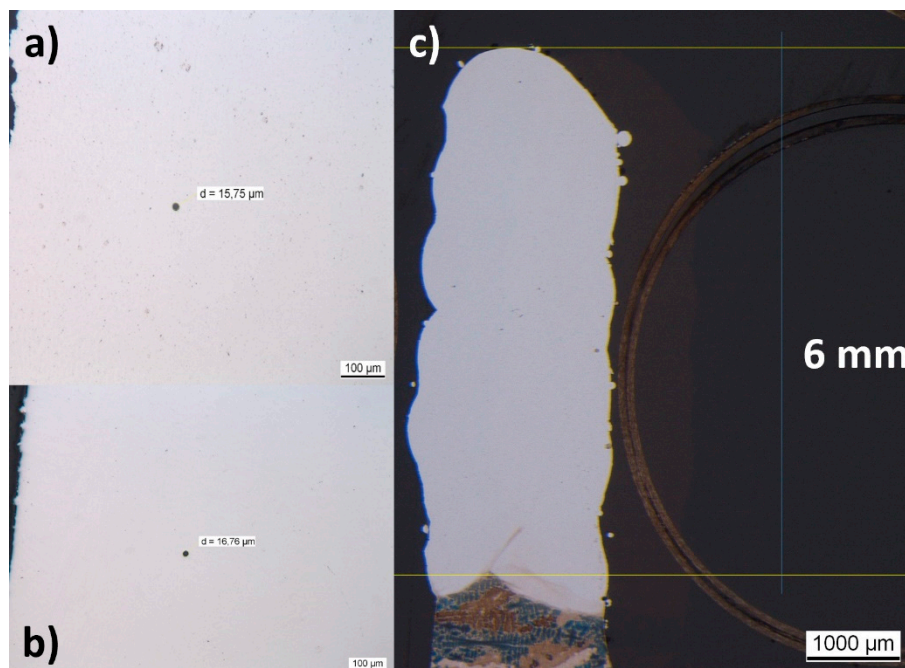


Figure 12. (a) Cross-section of a regenerated nickel-based turbine blade; (b) and (c) pores within the regenerated structure.

Typically, damaged blades are removed from the compression wheel for regeneration. However, some types of compression wheels have been produced with non-removable blades. The system developed here is able to cover these cases as well, since the shaft of the turbocharger is mounted in the turntable. The operator can select different blades to be reconditioned. Figure 13 shows the reconditioning process as applied to a turbocharger wheel with irresolvable blades.

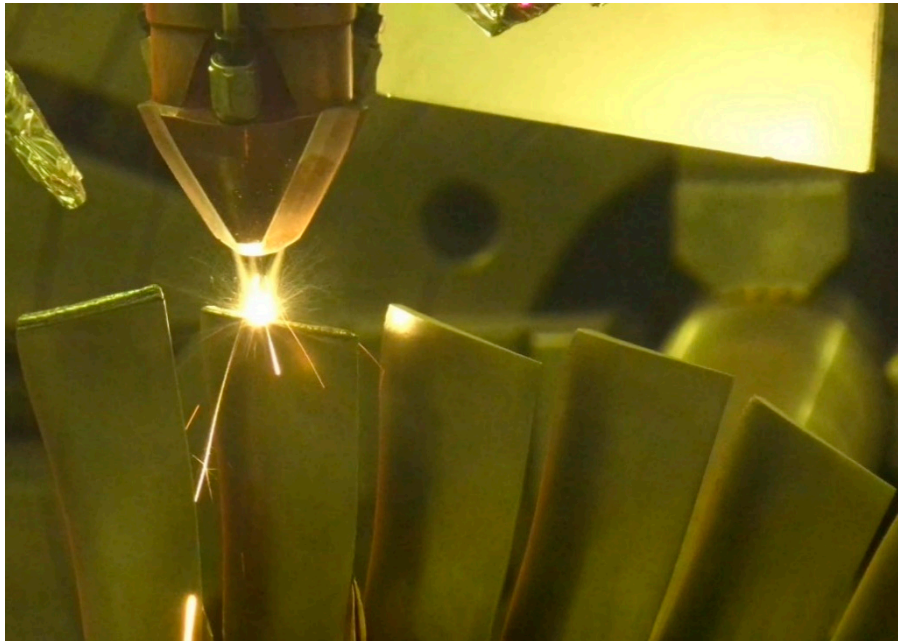


Figure 13. Reconditioning of blades.

The system developed within this project also offers economic advantages, helping make digitalization an interesting and affordable option for SMEs. It may generate time savings of about 70% compared to the teach-in method, as well as reducing workload and strain on the operator due to the potential for elimination of secondary steps such as checking distances, holding the dead-man switch while repositioning, and working in a bent-over position. Unlike the tactile method, the system developed within the project is applicable to parts regardless of their dimensions, as long as their thickness is covered by the width of the laser line. Major advantages of the system described here over the CAD/CAM solution include low initial recognition costs and the fact that the system dispenses with the need for an additional CAD/CAM workstation and with the cost of software licenses.

5. Conclusions

This project involved the development of a system which automatically identifies the area of a part to be reconditioned. The process creates a welding seam strategy without additional CAD software; it takes the inaccuracy of the handling system into account and thus promises reproducible quality. In addition, the project developed a solution for so-called zero-series production, enabling the processing of different geometries of components of the same type within one process. The mechanical properties of the reconditioned parts are comparable to those conventionally processed; the digitalization of the process gives rise to potential for higher productivity. Moreover, the system increases the attractiveness of a traditional area of industry to junior employees.

The system developed in this project reduces costs by at least 50% compared to manual teaching, depending on the component, as the installation at the project partner showed. As a result, components can now be repaired that would previously have been scrapped for cost reasons. At the same time, reworking was reduced, as the quality of the work does not depend on the performance of the specific employee. Initial implementation of the system in a business requires external assistance, which takes

three working days, including the requisite training, as long as minimum knowledge on how to move a robot is already in place. Due to the choice of scanner, components with a maximum width of 120 mm can currently be processed in a fully automated manner, as the system was primarily designed to recondition thin-walled components.

Author Contributions: Funding acquisition, Conceptualization, writing—original draft preparation, S.S.; methodology, formal analysis, software, E.M.; writing—review and editing, supervision, J.M.; validation, project administration, F.W. All authors have read and agreed to the published version of the manuscript.

Funding: This research was funded by the European Regional Development Fund (ERDF) and the Free and Hanseatic City of Hamburg, as part of the “Professional Transfer Plus” funding program (grant number 51077285).

Conflicts of Interest: The authors declare no conflict of interest.

References

1. Lindenhoven, W.; Suchodoll, D.; Küpper, H.; Hackel, M. *Automatisiertes 3D Auftragsschweißen von Bodenplatten*; Große Schweißtechnische Tagung: Basel, Switzerland, 2007; pp. 419–425.
2. Sheikhi, S. *Roboterbasierte Prozesse zur Schweißtechnischen Rekonditionierung von Komponenten im Schiffsbau, 18 Duisburger Schweisstage*; SLV-Duisburg: Duisburg, Germany, 2013.
3. Sheikhi, S. Neuer Standard: Regeneration von Großdieselmotorkomponenten durch Laserstrahl auftragschweißen. *Der Praktiker* **2012**, *64*, 546–551.
4. Drews, P.; Starke, G.; Hackel, M.; Kremer, S. *Automated Surface Welding for the Repair of Forming Tools, Wasmuht, Welding and Cutting 3*; ; DVS Verlag: Duisburg, Germany, 2004; p. 2428.
5. Hackel, M.; Starke, G. *Prozessintegrierte Werkstückdigitalisierung in der Bearbeitungszelle für Eine Effiziente Automatisierung Bei Kleiner Losgröße, Robotik*; Robotik 2004; VDI-Berichte: Düsseldorf, Germany, 2004; pp. 173–178. ISBN 3-18-091841-1.
6. Available online: <https://www.micro-epsilon.com/service/glossar/Laser-Linien-Triangulation.html> (accessed on 6 January 2020).
7. Jones, J.; McNutt, P.; Tosi, R.; Perry, C.; Wimpenny, D. Remanufacture of turbine blades by laser cladding, machining and in-process scanning in a single machine. In Proceedings of the 23rd Annual International Solid Freeform Fabrication Symposium, Austin, TX, USA, 6–8 August 2012.
8. Gorry, A. General least-squares smoothing and differentiation by the convolution (Savitzky–Golay) method. *Anal. Chem.* **1990**, *62*, 6. [[CrossRef](#)]
9. Nowotny, S.; Scharek, S.; Beyer, E.; Richter, K.H. Laser beam build-up welding: Precision in repair, surface cladding, and direct 3D metal deposition. *J. Therm. Spray Technol.* **2007**. [[CrossRef](#)]
10. Syed, W.U.H.; Pinkerton, A.J.; Li, L. Combining wire and coaxial powder feeding in laser direct metal deposition for rapid prototyping. *Appl. Surf. Sci.* **2006**, *252*, 4803–4808. [[CrossRef](#)]
11. Huang, J.; Li, Z.; Cui, H.; Yao, C.; Wu, Y. Laser welding and laser cladding of high performance materials. *Phys. Procedia* **2010**, *5*, 1–8. [[CrossRef](#)]
12. Xu, J.; Liu, W.; Kan, Y.; Zhong, M. Microstructure and wear properties of laser cladding Ti–Al–Fe–B coatings on AA2024 aluminum alloy. *Mater. Des.* **2006**, *27*, 405–410. [[CrossRef](#)]
13. Carcel, B.; Sampedro, J.; Ruescas, A.; Toneu, X. Corrosion and wear resistance improvement of magnesium alloys by laser cladding with Al–Si. *Phys. Procedia* **2011**, *12*, 353–363. [[CrossRef](#)]
14. Cao, X.; Jahazi, M.; Fournier, J.; Alain, M. Optimization of bead spacing during laser cladding of ZE41A–T5 magnesium alloy castings. *J. Mater. Process. Technol.* **2008**, *205*, 322–331. [[CrossRef](#)]
15. Zhang, K.; Zhang, X.M.; Liu, W.J. Influences of processing parameters on dilution ratio of laser cladding layer during laser metal deposition shaping. *Adv. Mater. Res.* **2012**, *549*, 785–789. [[CrossRef](#)]

